Supporting Information for

Interfacial Electrostatics of Poly(vinylamine hydrochloride), Poly(diallyldimethylammonium chloride), Poly-L-lysine, and Poly-L-arginine Interacting with Lipid Bilayers

McGeachy, A. C.,[a] Dalchand, N.,[a] Caudill, E. R.,[b] Li, T.,[a] Doğangün, M.,[a] Olenick, L. L.,[a] Chang, H.,[a] Pedersen, J.A., [b-e] Geiger, F.M.[a]

[a]Department of Chemistry, Northwestern University, 2145 Sheridan Road, Evanston, IL 60660

[b]Department of Chemistry, University of Wisconsin-Madison, 1101 University Avenue, Madison, WI 53706

[c]Environmental Chemistry and Technology Program, University of Wisconsin-Madison, 660 North Park Street, Madison, WI 53706

[d]Department of Soil Science, University of Wisconsin-Madison, 1525 Observatory Drive, Madison, WI 53706

[e]Department of Civil & Environmental Engineering, University of Wisconsin-Madison, 1415 Engineering Drive, Madison, WI 53706

1. Vesicle and Supported Lipid Bilayer Preparation Methods for Second Harmonic Generation Spectroscopy (SHG) Experiments.

A. Comparison of Lipid Vesicle Preparation and Lipid Bilayer Formation Methods. In this work two different methods for lipid vesicle preparation and supported lipid bilayer (SLB) were employed. The procedure for drying lipid films is consistent across Methods 1 and 2. Details of each method are outlined below:

Method 1

Lipid vesicle films are reconstituted with 0.1 M NaCl, 0.005 M $CaCl_2$ 0.01 M Tris buffer and gently warmed for 30 minutes. The reconstituted lipids were mechanically extruded through a polycarbonate membrane with a pore size of 0.05 μm at a lipid concentration of 2 mg/mL (Avanti Polar Lipids). The vesicle solutions were diluted to a final concentration of 0.5 mg/mL at 0.1 M NaCl, 0.01 M Tris, 0.005 M $CaCl_2$ and stored in a 5-mL polypropylene round bottom Falcon tubes at 4 °C (Method 1). The addition of divalent salts has been shown to facilitate the formation of lipid bilayers from vesicle containing solutions onto supportive substrates such as fused silica. However, addition of $CaCl_2$ to vesicles containing large amounts of anionic lipids has been shown to result in vesicle aggregation. We have previously shown that there is no noticeable aggregation of vesicles using Method 1.[1] The majority of experiments involving PVAm and PDADMAC (400-500 kDa) were performed using Method 1. In experiments performed with this method, the cell was equilibrated with 0.1 M NaCl, 0.01 M Tris buffer adjusted to pH 7.4. The vesicle containing solutions was then introduced into the flow cell at a flow rate of approximately 2 mL per minute. After allowing the bilayer to form over at least 15 minutes, the flow cell is then flushed with 20 mL of 0.1 M NaCl buffer (0.01 M Tris, pH 7.4). All experiments are performed at room temperature (~20 °C). Fluorescence recovery after photobleaching has shown that this method produces well-formed bilayers.[2]

Method 2

We also conducted a subset of experiments with lipids that were reconstituted instead with 0.001 M NaCl, 0.01 M Tris buffer, vortexed, and transferred to 2-mL microcentrifuge tubes. After vortexing, the lipids were sonicated (bath sonicator for 30 minutes) and then subjected to 3 freeze-thaw cycles (5-minute liquid N_2 and 5-minute thaw in bath sonicator) (Method 2). Method 2 for

vesicle preparation was also used primarily for SHG experiments with PDADMAC (100 kDa), PLL, and PLR. However, control experiments using this method for PVAm and PDADMAC (400 kDa) were also conducted. The vesicles were stored in a 2-mL microcentrifuge tube at 4 °C and diluted to a final concentration of 0.5 mg/mL at 0.15 M NaCl, 0.01 M Tris, 0.005 M $CaCl_2$ immediately before use for SHG experiments. In SHG experiments performed with this method, the SHG flow cell was equilibrated with 0.15 M NaCl, 0.01 M Tris, 0.005 M $CaCl_2$ buffer and then lipid suspensions were injected at a flow rate of 2 mL per minute. After allowing the bilayer to form over at least 15 minutes, the flow cell was flushed with 10 mL of 0.15 M NaCl, 0.01 M Tris, 0.005 M $CaCl_2$, 10 mL of 0.15 M NaCl, 0.01 M Tris, and finally 20 mL of 0.1 M NaCl, 0.01 M Tris buffer.

B. Fluorescence Recovery after Photobleaching (FRAP) Measurements. Fluorescence recovery after photobleaching (FRAP) is a fluorescence technique that provides insight into lipid surface coverage and the two dimensional lateral mobility of lipids within the silica-supported lipid bilayer. Diffusion coefficients, determined through FRAP measurements, have been used previously as a method for evaluating the quality of supported lipid bilayers.[1-3] Here, FRAP measurements were carried out in a manner consistent with our previously published work.[2] Specifically, we used a Leica Spinning Disk Microscope (Leica DMI6000 inverted microscope equipped with a Yokogawa CSU-X1 Spinning Disk module) with either a 40x or 63x oil immersion objective. The samples are visualized by a Photometrics Evolve Delta512 camera (60fps at 512 × 512 chip camera, 16 μm pixel size, backthinned electron multiplying charge coupled device). Photobleaching was carried out using an iLas[2] attachment from Roper Scientific which is mounted onto the microscope (401 nm 50 mW; 50-100% of laser power). Images were collected with the Green ET525/50M emission filter and 488 nm, 50 mW laser at 10-15% power.

Metamorph was used for data collection and ImageJ was used for data processing. The simFRAP plugin for ImageJ was used to extract lateral diffusion coefficients.[4]

For these experiments, the vesicles were doped with 0.1 mol% TopFluor PC® (Avanti Polar Lipids, 810281). Experiments were carried out in a similar manner as described in the main text, using a homebuilt Teflon flow cell, 1-inch diameter UV grade fused silica window (ISP Optics, QU-W-25-1) marked on the edge with marker (to facilitate aligning) and either Method 1 or Method 2 for vesicle preparation (T = 20-22°C). After forming the SLB in the Teflon flow cell at the silica/water interface, the SLB was rinsed with 20-mL of 0.1 M NaCl, 0.01 M Tris buffer solution adjusted to pH 7.4. The window was carefully removed and mounted into a modified closed cultivation cell (Pecon, POC-R2). To avoid disrupting the bilayer, the window is separated from the imaging window by a thin layer of silicone grease and a small reservoir of 0.1 M NaCl buffer.

For SLBs produced with Method 1, which did not employ the freeze-thaw pretreatment, we find an average diffusion coefficient of 0.6 ± 0.3 $\mu m^2/s$ (18 replicates over 6 individual samples). SLBs formed from Method 2 have an average diffusion coefficient of 1.4 ± 0.3 $\mu m^2/s$ (18 replicates over 2 individual samples). We also find that both methods discussed above produce SLBs with mixtures of liquid-crystalline and gel phase domains. As such, we find diffusion coefficients on the order of ~1 and ~0.01 $\mu m^2/s$ which corresponds to the liquid-crystalline and gel phase supported lipid bilayers, respectively. The diffusion coefficients reported here agree well with our previously reported estimates for diffusion coefficients of SLBs formed via Method 1.[2] Representative traces are shown in Figure S1. The error associated with the average diffusion coefficient is the standard error determined by dividing the standard deviation of the diffusion coefficients over all of the sample replicates by the square root of the number of replicates. We

have also provided the values of the diffusion coefficients for each individual replicate, along with their errors, in tabular form (Table S1).

C. SLB Preparation Methods Influence on Adsorption of Cationic Polymers. To understand the influence of a given vesicle preparation method and subsequent SLB formation method on the observed signal changes in our SHG experiments, we decided to conduct experiments using both methods (see above for details) for each polymer. Specifically, we wanted to qualitatively compare the impact of lipid bilayer preparation on the trends we observed in SHG adsorption isotherms. SFG studies seemed to indicate that bilayer preparation method could influence the interactions between PDADMAC (400-500 kDa) and SLBs formed from 9:1 DMPC/DMPG. To summarize the results from these experiments, we observe similar trends in our SHG studies as demonstrated by the reproducible decrease in SHG signal intensity with increasing polycation concentration (Figure S2).

2. Interactions of poly(vinyl alcohol) and poly(acrylic acid) with 9:1 DMPC/DMPG.

In an effort to 1) explore the generalizability of SHG as a tool for probing polymer interactions with supported lipid bilayers and 2) verify that the results that we obtained with polycations is not a general consequence of introducing polymers into the flow cell, we conducted SHG experiments with poly(vinyl alcohol) (PVOH) and poly(acrylic acid) (PAA). Unlike the polycations that are discussed in the main text, PVOH and PAA are neutral and negatively-charged, respectively. PAA and other polyanions complexed with lipids have applications in drug delivery[5] because of their ability to solubilize membrane surfaces in a tunable manner.[6,7] PVOH is considered to be nontoxic and has many applications including in nanocomposite films,[8] biocompatible nanomaterial coatings,[9] and the production of novel barrier materials.[10] In the studies discussed in the main text, which describe the interactions that occur between various polycationic polymers, we see ~10-30%

decreases in SHG *E*-fields. Upon interaction with PVOH with an average molecular weight of 9 or 85 kDa with supported lipid bilayers formed from 9:1 DMPC/DMPG at 0.1 M NaCl, we see negligible changes in SHG signal intensity with increasing polymer concentration. The absence of signal change in the presence of PVOH and small signal changes in the presence of PAA indicate that the signal changes that we observe in the interactions between polycations and SLBs formed from 9:1 DMPC/DMPG are not attributable to some general phenomenon that arises from the presence of *any* polymeric species. We also reduced performed these experiments with no added NaCl (I ~0.01 M with contributions from Tris buffer adjust to pH 7.4). We find that even with the reduced ionic strength, neutral polyvinyl alcohol does not cause a significant change in SHG signal intensity (Figure S3). From these experiments, we can support the interpretation of our results which we take to suggest that the adsorption of polycationic polymers to SLBs formed from 9:1 mixtures of DMPC and DMPG is due to changes in the overall interfacial potential and not a consequence of general exposure to polymeric materials.

3. Sum Frequency Generation Spectroscopy Studies of Polycation/SLB Interactions. Vibrational SFG spectroscopy is a useful tool for monitoring the structure and integrity of SLBs and has been used to explore bilayer asymmetrization and lipid flip-flop,[11-17] bilayer disruption, adsorption processes,[18] and domain formation.[19] As discussed in the main text, sum frequency generation spectroscopy (SFG) was used here as a tool for qualitatively evaluating the integrity of the SLBs before, during, and after interaction with polycationic polymers. Our SFG system has been described in the literature previously.[1,11,20,21] Briefly, SFG spectra are collected *via* a regeneratively amplified Ti:Sapphire laser system (SpectraPhysics) which pumps an optical parametric amplifier tuned to the C-H stretching region. An IR-grade fused silica window (ISP Optics, QI-W-25-3) was clamped onto a home-built Teflon flow cell fitted with a Viton O-ring,

creating a leak-tight seal. SFG spectra were recorded with four-minute integration times with five acquisitions at each center IR wavelength. The reported SFG spectra were all background-subtracted, calibrated to the characteristic vibrational modes of polystyrene in the C-H stretching region (2850 and 3060 cm^{-1}), and then normalized to the nonresonant sum frequency signal of a gold-coated fused silica window.

To explore the propensity of the polycations explored herein to cause significant disruptions to or alterations in the structure of SLBs formed from 9:1 mixtures of DMPC and DMPG, we employed SFG spectroscopy to monitor the spectral signatures from the C-H oscillators of the phospholipid alkyl chains and lipid headgroup between 2700 and 3200 cm^{-1} before, during, and after exposure to 50 nM polymer concentrations. SFG spectra of SLBs formed from 9:1 DMPC/DMPG at fused silica/water interfaces produce 3 signature features at 2875, 2907, and 2950 cm^{-1}.[1,11] Upon exposure of SLBs to 50 nM $PDADMAC_{400}$ at 0.1 M NaCl, we observe two peaks centered at 2950 and 2907 cm^{-1} when using Method 1. In experiments using Method 2, we observe a second outcome in which the original features are preserved, but have reduced SFG signal intensity. Control experiments indicate that the two peaks observed in experiments that do not utilize the freeze-thaw pretreatment after exposure to $PDADMAC_{400}$ polymer is not attributable to contributions from C-H oscillators associated with polymer present at the interface. The nature of these changes to SFG signal intensity upon interaction with $PDADMAC_{400}$ are the basis of ongoing work.

Previously, we have shown that concentrations of poly(allylamine hydrochloride) (PAH) in excess of 1 μM caused significant disruption to SLBs formed from 9:1 DMPC/DMPG in the initial phases of lipid corona formation, as indicated by a loss of spectral signatures associated with a well formed bilayer. Given the changes that can occur to the bilayer surface at high polycation

concentrations, our SHG experiments have been carried out in a concentration range that avoids the confounding impacts of polycation adsorption and bilayer disruption towards the interpretation of our SHG results. At and below the concentrations used in the SFG experiments carried out here, we observe that that the spectral features that we associate with a well-formed bilayer are preserved (Figure S4).

4. Quartz Crystal Microbalance with Dissipation Monitoring (QCM-D) Technique. QCM-D is a useful analytical tool for 1) monitoring the formation of supported lipid bilayers, 2) monitoring polymer-membrane interactions, and 3) quantifying the acoustic mass of adsorbed species (mass of adsorbed species plus hydrodynamically coupled water). We also used QCM-D as a mechanism for understanding the reversibility of polycation adsorption.

A. QCM-D Theory. Taking advantage of the piezoelectric properties of quartz, an alternating current is applied across an AT-cut quartz crystal which induces oscillations in the quartz crystal, and produces a standing shear wave between two electrodes. This shear wave decays into the bulk aqueous solution over a few hundred nm and the resonator frequency is sensitive to mass coupled to the oscillations of the sensor. In this technique both solvent viscosity and density, and mass changes can be observed by QCM-D. When the adsorbed mass is rigidly coupled to the oscillating sensor (taken as $\Delta D_v/(\Delta f_v/v) << 0.4 \times 10^{-6}$ Hz^{-1}, where ΔD_v and Δf_v are respectively the change in dissipation factor and change in resonance frequency for harmonic number v),[22] the adsorbed mass can be calculated using the Sauerbrey equation:[23]

$$\Delta\Gamma_{\text{QCM-D}} = -C\frac{\Delta f_v}{v} \qquad \text{S1}$$

where $\Delta\Gamma_{\text{QCM-D}}$ is the change in acoustic surface mass density which includes the mass of hydrodynamically coupled water and C is the mass sensitivity coefficient (18.0 ng·cm^{-2}·Hz^{-1} at the

fundamental frequency for the 4.95 MHz crystals used here). Data are reported for the 5th harmonic.

B. QCM-D as a Tool for Quantifying Mass Uptake to Bilayer Surfaces. Shifts in frequency are a useful metric for determining acoustic mass changes associated with adsorption processes. As indicated by Equation S1, a reduction in the frequency of oscillations in the quartz crystal as compared to an initial baseline frequency corresponds to a positive $\Delta\Gamma_{QCM\text{-}D}$ (acoustic surfaces mass density). Upon flowing polymer containing solutions, we observe negative shifts in frequency which corresponds to an increased mass on the quartz crystal. As discussed above, this mass, which we refer to as the acoustic mass, also includes the mass of water and counterions coupled with the polymer adsorbed to the surface. Normalized frequency changes for the 5th harmonic and acoustic masses of polycations adsorbed to 9:1 DMPC/DMPG during interaction and after interaction are reported in Figure S5 and presented in tabular form in Table S2.

As mentioned in the main text, in estimating the number density in terms of polymers over unit area (polymers/cm^2), we assume that approximately 31% of the acoustic mass reported from our QCM-D measurements is attributable to hydrodynamically coupled water. This assumed contribution of hydrodynamically coupled water to the overall reported acoustic mass is based on previous studies which describe the adsorption of an insecticidal protein to humic acid/PLL films supported on SiO_2 substrates[24] and is in line with reported water content of polymer multilayer films.[25] We acknowledge that the water content in the measured acoustic masses may differ from that reported in these previous studies. In an effort to better understand how this assumption influences the reported polymer number densities, in terms of polymers per unit area, and in our estimates for percent of ionized groups, we varied the percent of water contributing to the total mass in our calculations from 1% to 70% and present these values in Figure S6. Without

complementary data from other techniques such as optical waveguide lightmode spectroscopy, dual polarization interferometry, ellipsometry, or localized surface plasmon resonance, determination of the proportion of the acoustic mass that is attributable solely to adsorbed polymer is difficult. These polymer densities translate to charge densities (in terms of number of positive charges per unit area) of 10^{14}-10^{15} positive charges/cm^2 at 0.1 M NaCl. Applying the same treatment to our previously reported data for PAH adsorption to SLBs formed from 9:1 DMPC/DMPG,[21] we also find a charge density on the order of 10^{14} charges/cm^2 under the same experimental conditions.

5. Comparing Adsorption Models for Describing Polyelectrolyte/Membrane Interactions. In this work we qualitatively explored the ability of the Gouy-Chapman and triple layer models to describe the electrostatic behavior of our system and the Langmuir and Hill models to describe the adsorption behavior.

A. Electrical Triple Layer Model. Although Gouy-Chapman has been used previously to describe the electrostatic behavior of supported lipid bilayers in our work and elsewhere, here we explored the applicability of the electrical triple layer model towards understanding the electrical properties of the SLB. The electrical triple layer model describes an electrical double layer composed of two constant-capacitance layers and a diffuse layer as described in Equation S2

$$\Phi_0 = \frac{\sigma_0}{C_1} + \frac{\sigma_\beta - \sigma_0}{C_2} + \Phi_d \qquad \text{S2}$$

where $C_1$and $C_2$are the capacitances in the zero and β planes, $\sigma_0$is the surface charge density, $\sigma_\beta$is the charge density at the β-plane, and $\Phi_d$is the potential of the diffuse planes. It is assumed that Φ_d decays according to the Gouy-Chapman theory as shown in Equation S3

$$\Phi_d = \frac{2k_BT}{ze}\sinh^{-1}\left[\sigma\sqrt{8000k_BTN_AC_{elec}\varepsilon_0\varepsilon_R}\right] \qquad \text{S3}$$

where σ is the charge density, ε_0 is the permittivity in free space, $\varepsilon_m$is the relative permittivity, C_{elec} is the electrolyte concentration, $k_B$is the Boltzmann constant, N_A is Avogadro's number, T is the temperature, e is the elementary charge, and z is the valency of the screening ion (assuming a symmetric 1:1 electrolyte). Applying the same approach described in the main text and considering that the charge density is modulated by surface coverage, θ, we can combine Equations S2 and S3 and arrive at a triple layer expression for the SHG response (Equation S4).

$$E_{SHG} \propto A + B\left\{\frac{\sigma_{ads}}{C_2} + \frac{2k_BT}{ze}\sinh^{-1}\left((\sigma_0 + \sigma_{ads}\theta)\left(\frac{8.44\,M^{1/2}m^2C^{-1}}{\sqrt{M + C_{elec}}}\right)\right)\right\} \quad \text{S4}$$

In many studies of mineral surfaces, C_2 is typically assigned a value of 0.2 F/m^2.[26, 27] We have previously shown in a study of trivalent metal cations adsorbing to fused silica that varying the value of C_2 by as much as 50% around 0.2 F/m^2 had no appreciable impact on model results.[28] Here, we varied the value of C_2 from 0.1 to 10 and have summarized the influence of this value on the estimated charge density. Generally, we find that varying C_2 up to 10 F/m^2 has little to no impact on the estimated charge density (Figure S7).

B. Applying Combined Electrostatic and Adsorption Models. In assessing the best combination of models that describe both the adsorption and electrostatic models, we generated a matrix composed of four combined models of the form: 1) Gouy-Chapman and Langmuir, 2) Gouy-Chapman and Hill, 3) triple layer and Langmuir, and 4) triple layer and Hill. Experimental data was fitted with each of these four combined models and the summary of this data is presented in Table S3. All fitting is completed in Igor Pro 6.1 which uses an iterative data fitting technique and employs the Levenberg-Marquardt algorithm to find values for unknown coefficients.[29] In fitting the experimental data with a function with unknown coefficients, we aim to find values for the specified coefficients that minimize the value of Chi-square. Chi-square, defined as $\sum_i \left(\frac{y - y_i}{\sigma_i}\right)^2$,[29]

is a measure of the goodness of a fit and allows us to qualitatively compare the conformability of our experimental data to a given model. We caution that these values are not an absolute metric for determining that a model adequately describes experimental data. Instead, these values allow us to qualitatively compare several models to each other. Here, the model that best fits the experimental data will be associated with the lowest Chi-square values. We summarize these values in Table S3.

6. Influence of Intermittent versus Continuous Flow on SHG Reversibility. To understand what role, if any, the choice of flow (static/intermittent) versus continuous flow had on our observations in terms of both adsorption and reversibility, we conducted a second set of experiments where reversibility was investigated under continuous flow conditions. In these continuous flow experiments, the bilayer was formed as described in Section 1 and the SHG signal was collected over at least 45 minutes under static flow conditions. Then polymer solutions were flowed over 70 minutes at a flow rate to 2 mL/min. Finally, the SLB was rinsed with Tris buffer (0.1 M NaCl) for at least one hour (Figure S8). Though preliminary, we find that the on-rate remains consistent across experiments employing intermittent and continuous flow for polymers adsorbing to SLBs formed from 9:1 DMPC/DMPG. Moreover, we find that over the same time-scales, the same trends in reversibility are observed. Specifically, PDADMAC remains irreversibly adsorbed, while PVAm begins to show early signs of recovery in SHG signal intensity. These results are important in demonstrating that the choice of flow conditions may only play a small role in these systems. More studies are needed to determine whether this observation holds for other polymer-bilayer systems.

References.

1. J. M. Troiano, L. L. Olenick, T. R. Kuech, E. S. Melby, D. Hu, S. E. Lohse, A. C. Mensch, M. Dogangun, A. M. Vartanian, M. D. Torelli, E. Ehimiaghe, S. R. Walter, L. Fu, C. R. Anderton, Z. Zhu, H. Wang, G. Orr, C. J. Murphy, R. J. Hamers, J. A. Pedersen and F. M. Geiger, Direct Probes of 4 nm Diameter Gold Nanoparticles Interacting with Supported Lipid Bilayers, *J. Phys. Chem. C*, 2015, ***119*** 534-546.
2. L. L. Olenick, H. M. Chase, L. Fu, Y. Zhang, A. C. McGeachy, M. Dogangun, S. R. Walter, H.-f. Wang and F. M. Geiger, Single-component Supported Lipid Bilayers Probed using Broadband Nonlinear Optics, *Phys. Chem. Chem. Phys.*, 2017.
3. T. H. Anderson, Y. Min, K. L. Weirich, H. Zeng, D. Fygenson and J. N. Israelachvili, Formation of Supported Bilayers on Silica Substrates, *Langmuir*, 2009, **25**, 6997-7005.
4. D. Blumenthal, L. Goldstien, M. Edidin and L. A. Gheber, Universal Approach to FRAP Analysis of Arbitrary Bleaching Patterns, *Sci. Rep.*, 2015, **5**.
5. B. Munavirov, O. Gnezdilov, M. Rudakova, O. N. Antzutkin and A. Filippov, Interaction of Polyacrylic Acid with Lipid Bilayers: Effect of Polymer Mass, *Mag. Reson. Chem.*, 2013, **51**, 750-755.
6. Y. Y. Chieng and S. B. Chen, Interaction between Poly(acrylic acid) and Phospholipid Vesicles: Effect of pH, Concentration, and Molecular Weight, *J. Phys. Chem. B*, 2010, **114**, 4828-4835.
7. A. K. Berkovich, E. P. Lukashev and N. S. Melik-Nubarov, Dipole Potential as a Driving Force for the Membrane Insertion of Polyacrylic Acid in Slightly Acidic Milieu, *Biochim. Biophys. Acta, Biomembr.*, 2012, **1818**, 375-383.
8. B. Karthikeyan, Spectroscopic Studies on Ag-polyvinyl Alcohol Nanocomposite Films, *Physica B Condens. Matter*, 2005, **364**, 328-332.
9. M. Mahmoudi, A. Simchi and M. Imani, Cytotoxicity of Uncoated and Polyvinyl Alcohol Coated Superparamagnetic Iron Oxide Nanoparticles, *J. Phys. Chem. C*, 2009, **113**, 9573-9580.
10. S. Gupta, S. Sindhu, K. A. Varman, P. C. Ramamurthy and G. Madras, Hybrid Nanocomposite Films of Polyvinyl Alcohol and ZnO as Interactive Gas Barrier Layers for Electronics Device Passivation, *RSC Advances*, 2012, **2**, 11536-11543.
11. M. Dogangun, M. N. Hang, J. M. Troiano, A. C. McGeachy, E. S. Melby, J. A. Pedersen, R. J. Hamers and F. M. Geiger, Alteration of Membrane Compositional Asymmetry by LiCoO2 Nanosheets, *ACS Nano*, 2015, **9**, 8755-8765.
12. J. S. Allhusen and J. C. Conboy, The Ins and Outs of Lipid Flip-Flop, *Acc. Chem. Res.*, 2017, **50**, 58-65.
13. T. C. Anglin and J. C. Conboy, Kinetics and Thermodynamics of Flip-Flop in Binary Phospholipid Membranes Measured by Sum-Frequency Vibrational Spectroscopy, *Biochemistry*, 2009, **48**, 10220-10234.
14. T. C. Anglin, K. Brown and J. C. Conboy, in *XXII International Conference on Raman Spectroscopy*, eds. P. M. Champion and L. D. Ziegler, 2010, vol. 1267, pp. 119-120.
15. J. C. Conboy and J. Liu, Membrane Lipid Flip-flop and More: The Structural and Thermodynamic Properties of Supported Lipid Membranes Measured by Sum-frequency Vibrational Spectroscopy, *Abstr. Pap. Am. Chem. Soc.*, 2004, **227**, U872-U872.

16. J. C. Conboy, New Analytical Approach to Measuring Lipid Flip-Flop in Phospholipid Bilayers: Direct Measurement of Membrane Asymmetry using Sum-frequency Vibrational Spectroscopy, *Abstr. Pap. Am. Chem. Soc.*, 2005, **229**, U138-U138.
17. C. Zhang, F. G. Wu, P. P. Hu and Z. Chen, Interaction of Polyethylenimine with Model Cell Membranes Studied by Linear and Nonlinear Spectroscopic Techniques, *J. Phys. Chem. C*, 2014, **118**, 12195-12205.
18. R. J. Feng, L. Lin, Y. Y. Li, M. H. Liu, Y. Guo and Z. Zhang, Effect of Ca2+ to Sphingomyelin Investigated by Sum Frequency Generation Vibrational Spectroscopy, *Biophys. J.*, 2017, **112**, 2173-2183.
19. J. J. Tan, S. J. Ye and Y. Luo, Observing Peptide-Induced Lipid Accumulation in a Single-Component Zwitterionic Lipid Bilayer, *J. Phys. Chem. C*, 2015, **119**, 28523-28529.
20. J. M. Troiano, T. R. Kuech, A. M. Vartanian, M. D. Torelli, A. Sen, L. M. Jacob, R. J. Hamers, C. J. Murphy, J. A. Pedersen and F. M. Geiger, On Electronic and Charge Interference in Second Harmonic Generation Responses from Gold Metal Nanoparticles at Supported Lipid Bilayers, *J. Phys. Chem. C*, 2016, **120**, 20659-20667.
21. J. M. Troiano, A. C. McGeachy, L. L. Olenick, D. Fang, D. Liang, J. Hong, T. R. Kuech, E. R. Caudill, J. A. Pedersen, Q. Cui and F. M. Geiger, Quantifying the Electrostatics of Polycation–Lipid Bilayer Interactions, *J. Am. Chem. Soc.*, 2017.
22. I. Reviakine, D. Johannsmann and R. P. Richter, Hearing What You Cannot See and Visualizing What You Hear: Interpreting Quartz Crystal Microbalance Data from Solvated Interfaces, *Anal. Chem.*, 2011, **83**, 8838-8848.
23. G. Sauerbrey, Verwendung von Schwingquarzen zur Wägung dünner Schichten und zur Mikrowägung, *Zeitschrift für Physik*, 1959, **155**, 206-222.
24. M. Sander, J. E. Tomaszewski, M. Madliger and R. P. Schwarzenbach, Adsorption of Insecticidal Cry1Ab Protein to Humic Substances. 1. Experimental Approach and Mechanistic Aspects, *Environ. Sci. Technol.*, 2012, **46**, 9923-9931.
25. J. J. I. Ramos, S. Stahl, R. P. Richter and S. E. Moya, Water Content and Buildup of Poly(diallyldimethylammonium chloride)/Poly(sodium 4-styrenesulfonate) and Poly(allylamine hydrochloride)/Poly(sodium 4-styrenesulfonate) Polyelectrolyte Multilayers Studied by an in Situ Combination of a Quartz Crystal Microbalance with Dissipation Monitoring and Spectroscopic Ellipsometry, *Macromolecules*, 2010, **43**, 9063-9070.
26. P. Leroy and A. Revil, A Triple-layer Model of the Surface Electrochemical Properties of Clay Minerals, *J. Colloid Interface Sci.*, 2004, **270**, 371-380.
27. J. N. Malin, P. L. Hayes and F. M. Geiger, Interactions of Ca, Zn, and Cd Ions at Buried Solid/Water Interfaces Studied by Second Harmonic Generation, *J. Phys. Chem. C*, 2009, **113**, 2041-2052.
28. D. S. Jordan, J. N. Malin and F. M. Geiger, Interactions of Al(III), La(III), Gd(III), and Lu(III) with the Fused Silica/Water Interface Studied by Second Harmonic Generation, *Environ. Sci. Technol.*, 2010, **44**, 5862-5867.
29. IGOR Pro Version 6.1 User Manual. Wavemetrics, Inc: Lake Oswego, OR: 2009.

Figure Captions.

Figure S1. Representative simFRAP plots of normalized fluorescence intensity as a function of time for SLBs formed from 9:1 DMPC/DMPG for Method 1 (top) and Method 2 (bottom).

Figure S2. Normalized SHG *E*-field as a function of polymer concentration, in molarity, at 0.1 M NaCl, 0.01 M Tris, pH 7.4 for (a) $PDADMAC_{400}$, (b) $PDADMAC_{100}$, (c) PVAm, (d) PLL, and (e) PLR. SHG *E*-field is normalized to the SHG *E*-field associated with the supported lipid bilayer formed from 9:1 DMPC/DMPG prior to exposure to polymer. Filled circles all indicate experiments completed with lipid vesicle preparation detailed in Method 1 (see Section S1A for more details). Open circles are experiments completed with vesicle preparation Method 2 (see Section S1A for more details). Each trial is indicated by different colored opened or filled circles.

Figure S3. Normalized SHG *E*-field as a function of polymer concentration, in molarity, at 0.1 M NaCl (filled circles) or no added salt (I = ~0.01 M with contributions from Tris buffer), 0.01 M Tris, pH 7.4 polyacrylic acid (PAA) and poly(vinyl alcohol). SHG *E*-field is normalized to the SHG *E*-field associated with the supported lipid bilayer formed from 9:1 DMPC/DMPG prior to exposure to polymer.

Figure S4. Normalized *ssp*-polarized SFG spectra of supported lipid bilayers formed from 9:1 DMPC/DMPG at 0.1 M NaCl (0.01 M Tris, pH 7.4) before (black, offset by 100), during (colored, offset by 50), and after (gray) exposure to (a) 50 nM $PDADMAC_{400}$, (a) 50 nM $PDADMAC_{100}$, (c) 50 nM PVAm, (d) 500 nM PLL, and (e) 500 nM PLR. SFG signal is associated with contributions from CH oscillators originating from alkyl chains of lipid tails.

Figure S5. Acoustic surface mass densities (ng/cm^2) for during (solid) and after (dashed) exposure to polymer at the indicated polymer concentrations (0.1 M NaCl, 0.01 M Tris, pH 7.4).

Figure S6. (a) Number density expressed as polymers/cm^2 and (b) percent of ionization (the number of ionizable groups carrying charge under these conditions) as a function of the fraction of total mass that is attributable to the mass of water contributing to the acoustic surface mass density.

Figure S7. Charge density determined from fitting SHG adsorption isotherms with a combined Hill and Triple Layer model to describe the adsorption process of polymer to supported lipid bilayers formed from 9:1 DMPC/DMPG at 0.1 M NaCl (0.01 M Tris, pH 7.4) as a function of choice for input C_2 value (see main text of Supporting Information for discussion). Inset: Charge densities as a function of choice of C_2 values between 0.1 and 1.

Figure S8. Normalized SHG *E*-field as a function of time in the presence SLBs formed from 9:1 DMPC/DMPG for 50 nM $PDADMAC_{400}$ (dark purple), 50 nM $PDADMAC_{100}$ (light purple), 500 nM PLL (light green), 500 nM PLR (red), and 50 nM PVAm (teal) at 0.1 M NaCl, 0.01 M Tris, pH 7.4. At $t = 0$, the supported lipid bilayer is unperturbed and the SHG signal is monitored at 0.1 M NaCl. At $t = 43$ min, polymer solution is introduced into the flow cell and at $t = 112$ min the flow cell is rinsed with polymer-free solution composed of 0.1 M NaCl, 0.01 M Tris, pH 7.4. Dashed colored lines are experiments employing continuous flow while solid colored lines (reproduced from Figure 2 in the main text) use intermittent flow.

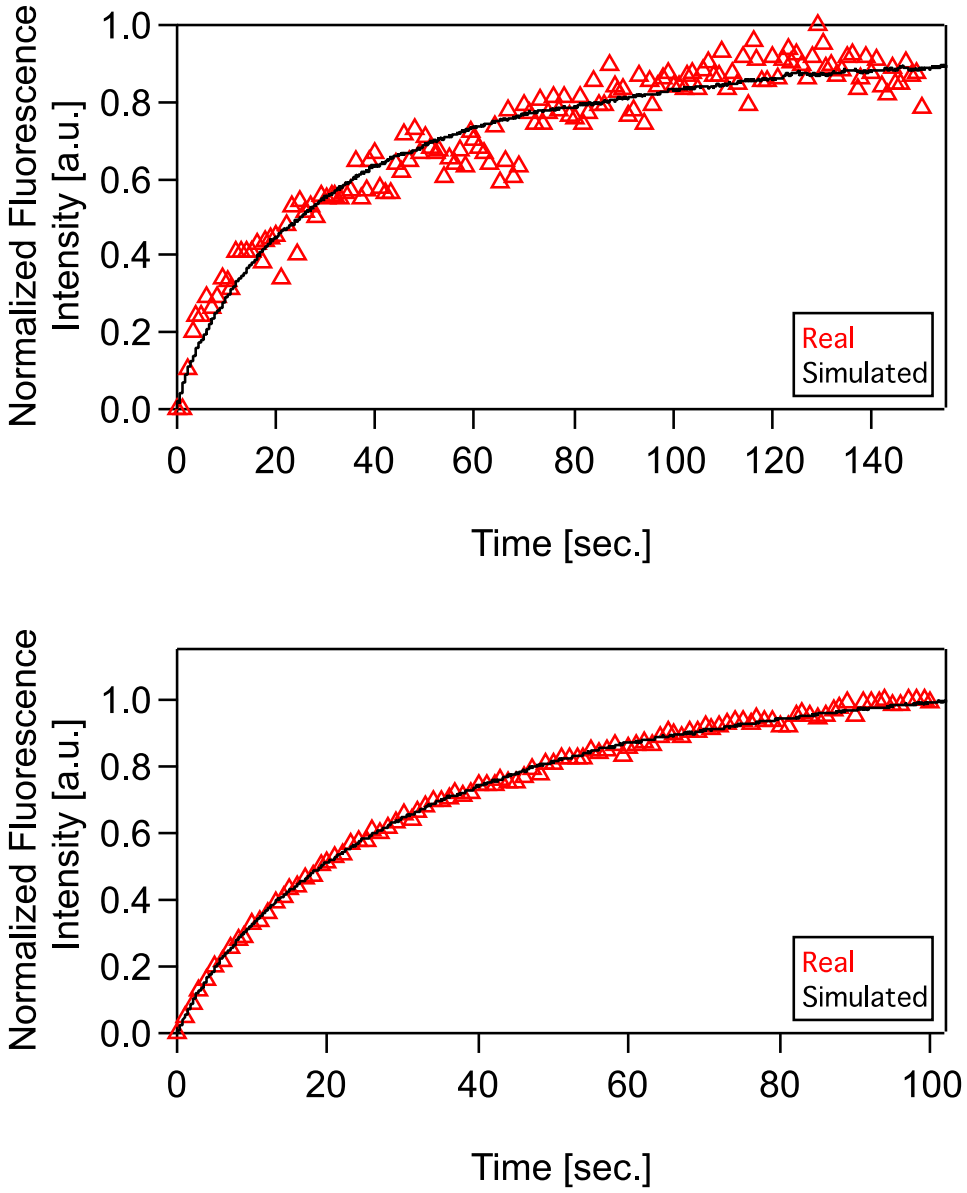
Normalized Fluorescence Intensity [a.u.]
1.0
0.8
0.6
0.4
0.2
0.0
0
20
40
60
80
100
120
140
Time [sec.]
Real
Simulated
Normalized Fluorescence Intensity [a.u.]
1.0
0.8
0.6
0.4
0.2
0.0
0
20
40
60
80
100
Time [sec.]
Real
Simulated

Figure S1.

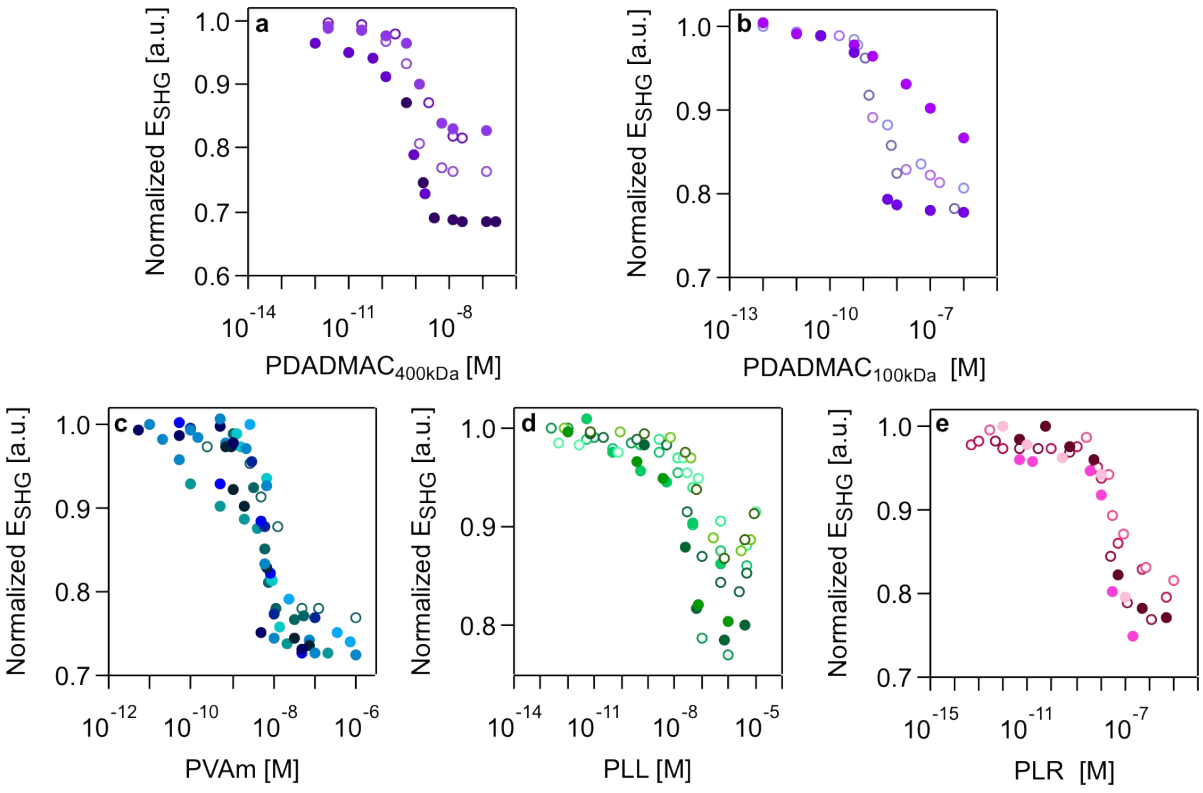
a
b
c
d
e
Normalized E_{SHG} [a.u.]
1.0
0.9
0.8
0.7
0.6
10^{-14}
10^{-11}
10^{-8}
PDADMAC$_{400kDa}$ [M]
10^{-13}
10^{-10}
10^{-7}
PDADMAC$_{100kDa}$ [M]
10^{-12}
10^{-10}
10^{-8}
10^{-6}
PVAm [M]
10^{-14}
10^{-11}
10^{-8}
10^{-5}
PLL [M]
10^{-15}
10^{-11}
10^{-7}
PLR [M]

Figure S2.

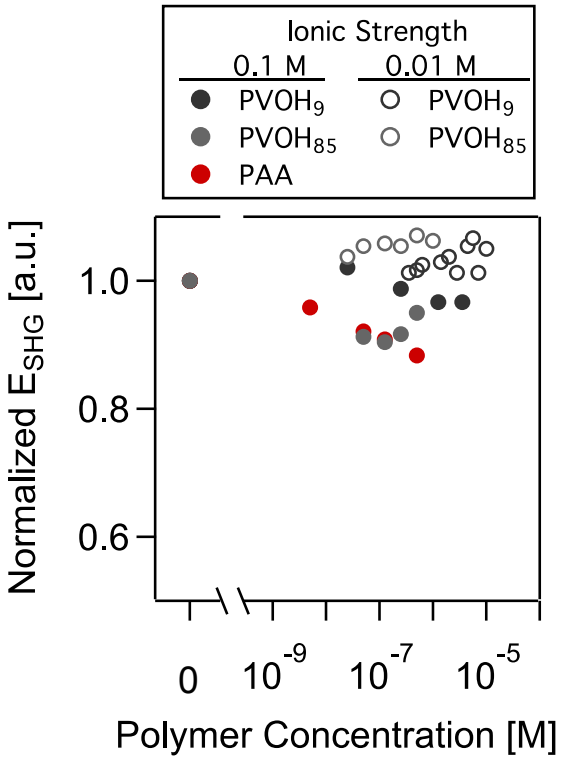
Ionic Strength
0.1 M
0.01 M
PVOH9
PVOH85
PAA
PVOH9
PVOH85
Normalized ESHG [a.u.]
1.0
0.8
0.6
0
10-9
10-7
10-5
Polymer Concentration [M]

Figure S3.

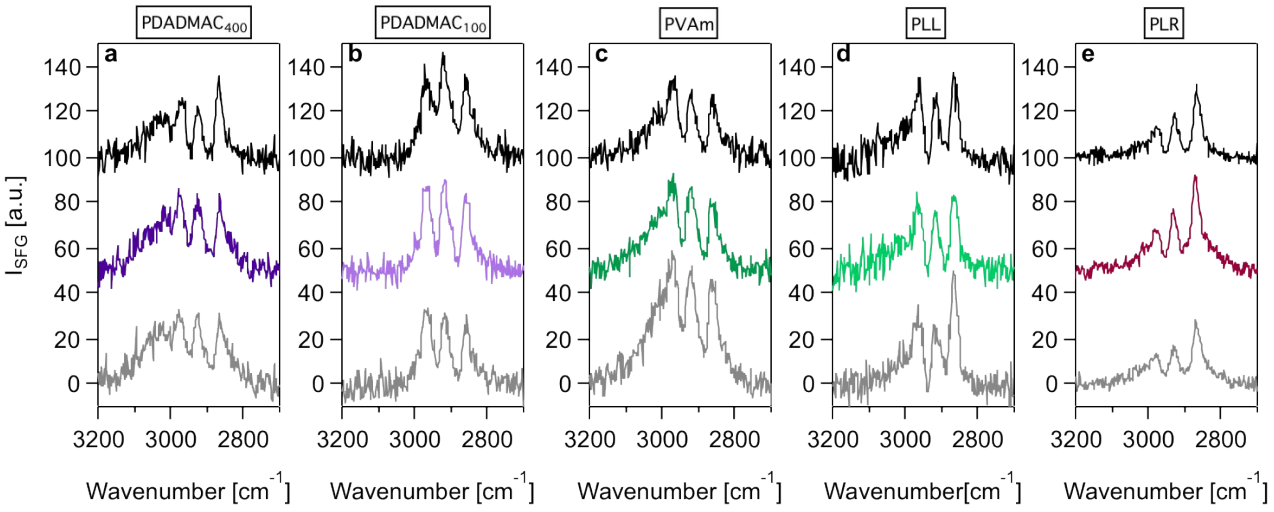
PDADMAC400
PDADMAC100
PVAm
PLL
PLR
a
b
c
d
e
ISFG [a.u.]
140
120
100
80
60
40
20
0
3200 3000 2800
Wavenumber [cm-1]
Wavenumber[cm-1]

Figure S4.

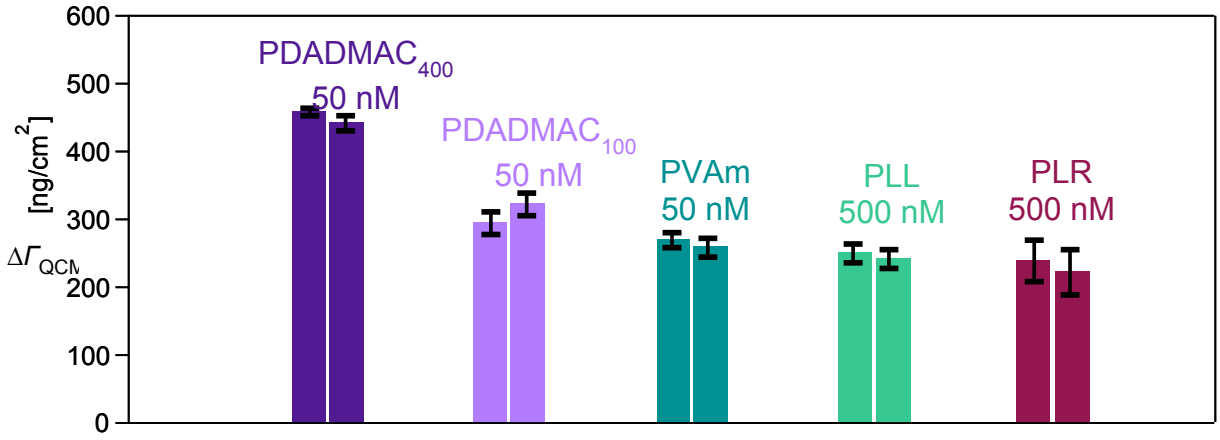
600
500
400
300
200
100
0
[ng/cm^2]
$\Delta\Gamma_{QCM}$
PDADMAC$_{400}$
50 nM
PDADMAC$_{100}$
50 nM
PVAm
50 nM
PLL
500 nM
PLR
500 nM

Figure S5.

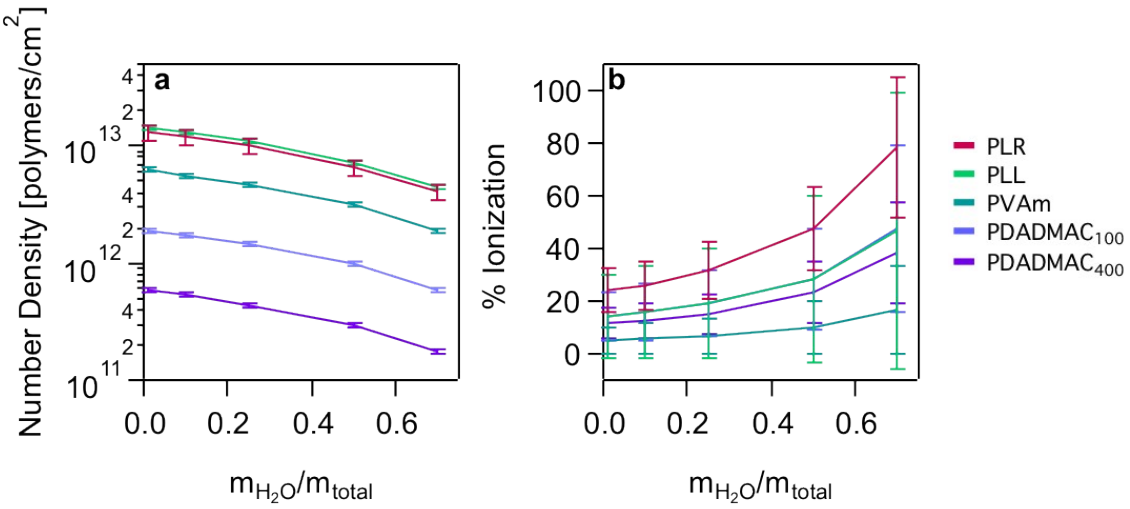
a
b
Number Density [polymers/cm^2]
% Ionization
m_{H_2O}/m_{total}
m_{H_2O}/m_{total}
PLR
PLL
PVAm
PDADMAC$_{100}$
PDADMAC$_{400}$

Figure S6.

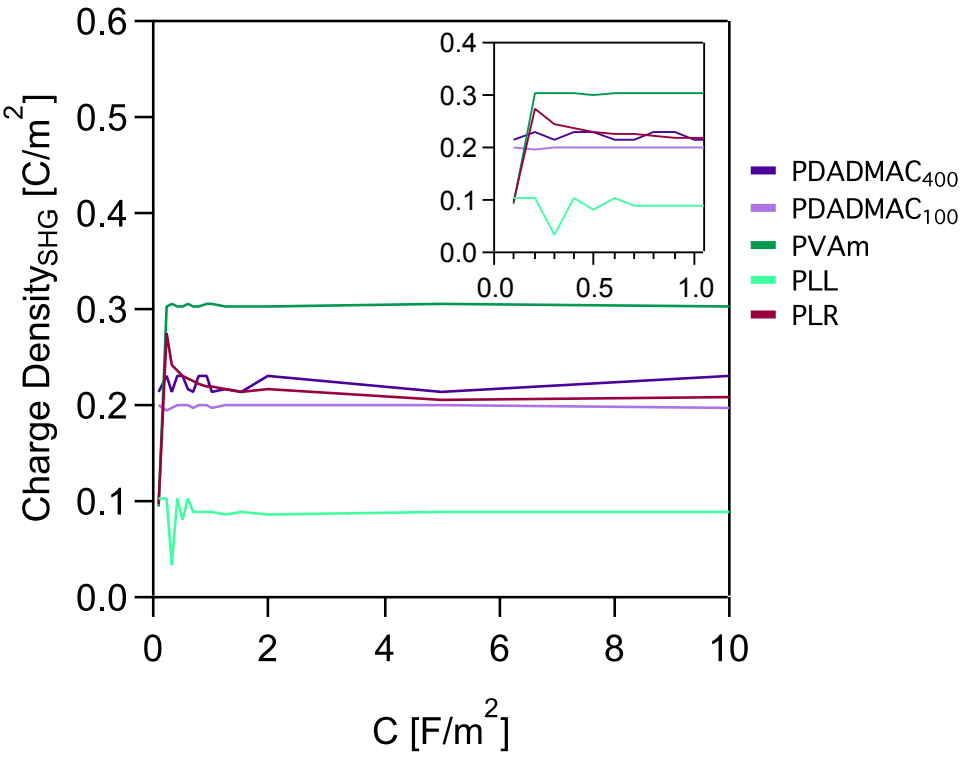
Charge Density$_{SHG}$ [C/m^2]
C [F/m^2]
0.0
0.1
0.2
0.3
0.4
0.5
0.6
0
2
4
6
8
10
0.0
0.1
0.2
0.3
0.4
0.5
1.0
PDADMAC$_{400}$
PDADMAC$_{100}$
PVAm
PLL
PLR

Figure S7.

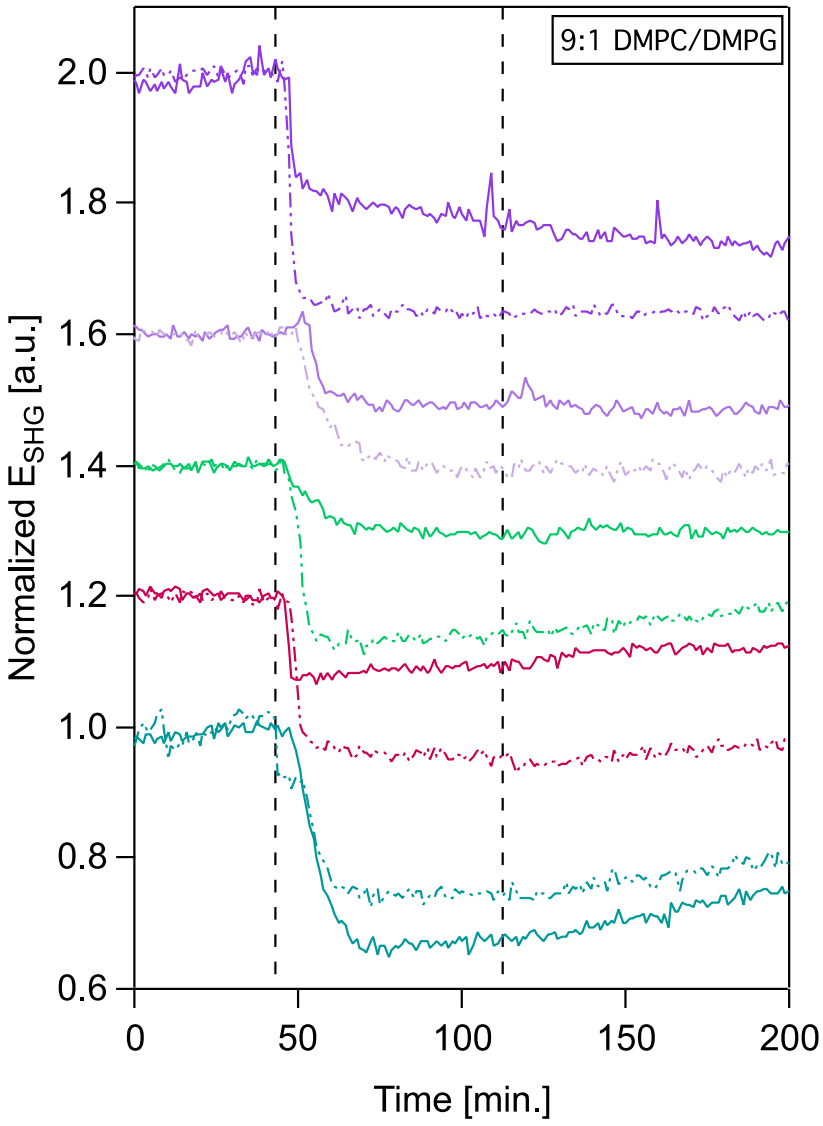
9:1 DMPC/DMPG
Normalized E_{SHG} [a.u.]
2.0
1.8
1.6
1.4
1.2
1.0
0.8
0.6
0
50
100
150
200
Time [min.]

Figure S8.

Table S1. Diffusion Coefficients (*D*) from Individual Replicates for SLBs formed *via* Methods 1 and Method 2.

Method 1 *D* [μm²/s]	Method 2 *D* [μm²/s]
0.27 ± 0.04	1.72 ± 0.04 [a]
0.15 ± 0.03	1.42 ± 0.06
5.4 ± 1.2	1.14 ± 0.05
0.047 ± 0.003	1.58 ± 0.06
0.92 ± 0.11	2.33 ± 0.07
0.68 ± 0.07[a]	1.01 ± 0.04
0.75 ± 0.18	1.50 ± 0.06
0.94 ± 1.7	0.62 ± 0.01
0.08 ± 0.01	0.31 ± 0.03
0.04 ± 0.01	0.026 ± 0.002
0.48 ± 0.21	0.066 ± 0.005
0.26 ± 0.01	3.5 ± 2.2
0.31 ± 0.01	2.1 ± 1.5
0.27 ± 0.01	4.2 ± 4.0
0.20 ± 0.01	0.57 ± 0.04
0.081 ± 0.006	1.3 ± 0.5
0.33 ± 0.07	1.9 ± 0.5
0.18 ± 0.02	0.58 ± 0.13

[a]This data is represented as a fluorescence recovery curve in Figure S1.

Table S2. Summary of Acoustic Masses as Reported by QCM-D (5th Harmonic) Before (Δm_{max}) and After (Δm_{rinsed}) Rinsing.

	polymer concentration (nM)	Δm_{max}	Δm_{rinsed}	*n*
PVAm	50	269 ± 12	259 ± 14	4
$PDADMAC_{100}$	50	294 ± 18	321 ± 16	3
$PDADMAC_{400}$	50	458 ± 5	442 ± 12	3
PLL	500	250 ± 15	242 ± 13	4
PLR	500	238 ± 31	222 ± 34	3

Table S3. Summary of Estimates for Charge Densities (σ) and Apparent Equilibrium Constants Yielded from Different Adsorption Models.

		GC+Langmuir	GC+Hill	TL+Langmuir[a]	TL+Hill[a]
PDADMAC$_{400}$	K [M^{-1}]	1.3 (± 0.5) × 10^{9}	9.5 (± 6.1) × 10^{8}	2.6 (± 0.4) × 10^{9}	2.3 (± 0.6) × 10^{9}
	σ [C/m^2]	0.25 ± 0.09	0.30 ± 0.15	0.32 ± 0.19	0.24 ± 0.23
	n	–	0.92 ± 0.09	–	1.24 ± 0.22
	χ^2	2.49 × 10^{-4}	2.20 × 10^{-4}	6.28 × 10^{-4}	6.27 × 10^{-4}
PDADMAC$_{100}$	K [M^{-1}]	3.5 (± 1.3) × 10^{8}	2.3 (± 2.1) × 10^{8}	6.4 (± 0.7) × 10^{8}	5.7 (± 1.2) × 10^{8}
	σ [C/m^2]	0.20 ± 0.06	0.28 ± 0.18	0.24 ± 0.05	0.20 ± 0.08
	n	–	0.92 ± 0.14	–	1.1 ± 0.16
	χ^2	2.00 × 10^{-4}	1.96 × 10^{-4}	2.12 × 10^{-4}	1.65 × 10^{-4}
PVAm	K [M^{-1}]	9.6 (± 49) × 10^{7}	1.7 (± 0.7) × 10^{8}	2.8 (± 0.6) × 10^{8}	1.8 (± 0.1) × 10^{8}
	σ [C/m^2]	0.11 ± 1.0	0.16 ± 0.15	0.47 ± 0.27	0.30 ± 0.05
	n	–	2.3 ± 1.0	–	2.9 ± 0.3
	χ^2	9.9× 10^{-3}	1.74 × 10^{-3}	7.69× 10^{-3}	1.17 × 10^{-3}
PLL	K [M^{-1}]	1.2 (± 1.3) × 10^{7}	2.6 (± 2.1) × 10^{7}	1.6 (± 0.7) × 10^{7}	2.8 (± 2.1) × 10^{7}
	σ [C/m^2]	0.35 ± 0.35	0.18 ± 0.20	0.17 ± 0.42	0.08 ± 0.34
	n	–	1.6 ± 0.76	–	2.2 ± 1.3
	χ^2	3.54 × 10^{-4}	2.52 × 10^{-4}	8.21 × 10^{-4}	2.78 × 10^{-4}
PLR	K [M^{-1}]	4.4 (± 0.5) × 10^{7}	2.8 (± 1.4) × 10^{7}	3.4 (± 0.8) × 10^{7}	3.6 (± 0.3) × 10^{7}
	σ [C/m^2]	0.17 ± 0.02	0.24 ± 0.08	0.23 ± 0.26	0.24 ± 0.20
	n	–	0.89 ± 0.08	–	1.28 ± 0.05
	χ^2	4.08 × 10^{-5}	4.40 × 10^{-5}	2.00 × 10^{-4}	3.00 × 10^{-5}

[a] C_2 is assigned a value of 0.2 F/m^2 (see main text of Supporting Information for discussion)